Title	DNA double-strand breaks induce the expression of flavin-containing monooxygenase and reduce root meristem size in Arabidopsis thaliana
Author(s)	Poyu Chen, Masaaki Umeda
Citation	Genes to Cells,20(8):636-646
Issue Date	29 May 2015
Resource Version	Author
Rights	© 2015 The Molecular Biology Society of Japan and Wiley Publishing Asia Pty Ltd This is the peer reviewed version of the following article: [Genes to Cells, 20(8):636-646], which has been published in final form at [https://doi.org/10.1111/gtc.12255]. This article may be used for non-commercial purposes in accordance with Wiley Terms and Conditions for Use of Self-Archived Versions.
DOI	10.1111/gtc.12255
URL	http://hdl.handle.net/10061/12587

DNA double-strand breaks induce the expression of flavin-containing monooxygenase and reduce root meristem size in *Arabidopsis thaliana*

Poyu Chen[1] and Masaaki Umeda[1,2]*

[1]Graduate School of Biological Sciences, Nara Institute of Science and Technology, 8916-5 Takayama, Ikoma, Nara 630-0192, Japan; [2]JST, CREST, 8916-5 Takayama, Ikoma, Nara 630-0192, Japan

***Correspondence:** Masaaki Umeda (E-mail: mumeda@bs.naist.jp)

Short title: ROS production in DNA damage response

Keywords: DNA damage, DNA double-strand breaks, Root meristem, Reactive oxygen species (ROS), Hydrogen peroxide (H_2O_2), *Arabidopsis thaliana*

Abstract

Plants utilize various mechanisms to cope with environmental stresses, which often threaten genome integrity. In *Arabidopsis*, DNA double-strand breaks (DSBs) reduce root meristem size in a SOG1-dependant manner. SOG1 is a key transcription factor controlling the response to DNA damage. However, the underlying mechanism remains largely unknown. In this study, we found that treatment with the DSB inducer zeocin increased the accumulation of H_2O_2 in root tips. Chromatin immunoprecipitation analysis revealed that SOG1 directly binds to the promoter of *FMO1*, which encodes a flavin-containing monooxygenase and is associated with the production of reactive oxygen species (ROS), H_2O_2 in particular. Indeed, zeocin induced the expression of *FMO1* in a SOG1-dependent manner, and neither the *sog1* nor the *fmo1* knockout mutant exhibited higher H_2O_2 accumulation in root tips. Consequently, both *sog1* and *fmo1* could tolerate exposure to zeocin, in terms of root growth and the maintenance of the meristem size. However, transgenic plants overexpressing *FMO1* also accumulated H_2O_2 in response to zeocin exposure, suggesting that other ROS-synthesis genes are also involved in the regulation of ROS production. We conclude that SOG1-mediated regulation of ROS homeostasis plays a key role in the reduction of root meristem size under DNA stress conditions.

Introduction

DNA damage induces gene mutations when the DNA repair system does not function properly. Thus, the regulatory mechanisms underlying the DNA damage response are an important part of maintaining genome integrity during plant development (Harper & Elledge 2007). DNA lesions are sensed by the sensor kinases ATM (ataxia telangiectasia mutated), and ATR (ATM and Rad3-related), which are activated by DNA double- and single-strand breaks, respectively (Riballo *et al.* 2004; Shiotani & Zou 2009). In mammals, CHK1 and CHK2 kinases are the downstream targets of ATM/ATR, and reduce cyclin-dependent kinases (CDK) activities in multiple ways; for example, they phosphorylate and stabilize the p53 transcription factor, which then induces the expression of the CDK inhibitor p21 (Riley *et al.* 2008). Reduction of CDK activities delays or arrests cell cycle progression, and allows cells to perform DNA repair prior to replication or mitosis (Zhou & Elldge 2000). Plants also possess ATM and ATR (Garcia *et al.* 2003; Culligan *et al.* 2004), but not downstream regulators such as CHK1, CHK2, and p53. Instead, the plant-specific transcription factor SOG1 (suppressor of gamma response 1) was identified in *Arabidopsis,* and is shown to play a major role in the DNA damage response downstream of ATM and ATR (Yoshiyama *et al*. 2009). The *sog1-1* mutant is tolerant of genotoxic stresses that cause DNA double-strand breaks (DSBs) because of its inability to arrest the cell cycle upon DNA damage (Yoshiyama *et al*. 2009; Adachi *et al*. 2011). We have recently reported that ATM directly phosphorylates and activates SOG1, inducing the downstream genes that trigger cell cycle arrest, DNA repair, cell death, and DNA polyploidization (Yoshiyama *et al*. 2013; Adachi *et al*.

2011). In fact, the genes coding for the CDK inhibitors SMR5 and SMR7 were found to be the direct targets of SOG1 (Yi *et al*. 2014).

In plants, DNA damage is caused by various stresses, such as high levels of aluminum or boron and pathogen infection (Nezames *et al.* 2012; Sakamoto *et al.* 2011; Yan *et al.* 2013). Reactive oxygen species (ROS), which are inevitable by-products of oxidative metabolism, redox-cycling events, and Fenton reactions, also cause DNA damage (Tanaka *et al.* 2006; Roldán-Arjona *et al*. 2009). Plasma membrane-localized NADPH oxidase produces superoxide ($O_2^{\bullet-}$) from molecular oxygen by using NADPH as an electron donor (Reeves *et al*. 2002). *Arabidopsis* has 10 genes for Atrboh (*Arabidopsis thaliana* respiratory burst oxidase homologues), all of them orthologues of the transmembrane subunit of mammalian NADPH oxidase (Foreman *et al*. 2003). Pathogen attack is known to activate Atrboh D and Atrboh F, and generate a high level of ROS via an oxidative burst, causing hypersensitive cell death (Torres *et al*. 2002; Mur *et al*. 2005). $O_2^{\bullet-}$ is transformed into H_2O_2 by superoxide dismutase (SOD), which is more stable than other ROS (Kovtun *et al.* 2000).

Although ROS injure cellular components such as DNA, they are also associated with the control of plant growth and development. For example, localized ROS production is observed at the apex of growing root hairs and pollen tubes, and are essential for tip growth (Takeda *et al*. 2008; Potocky *et al*. 2007). It is also known that ROS homeostasis is important for controlling root growth; namely, $O_2^{\bullet-}$ accumulates in the meristematic zone (MZ), while H_2O_2 accumulates in the elongation/differentiation zone (EDZ) (Dunand *et al*. 2007; Tsukagoshi *et al*. 2010). In *Arabidopsis*, the

transcription factor UPB1 suppresses the expression of peroxidase, which reduces H_2O_2 molecules to water at the boundary between the MZ and the EDZ. It has been suggested that UPB1 is involved in H_2O_2 accumulation in the EDZ, and controls $O_2^{\bullet-}$ and H_2O_2 distribution, thus affecting meristem size and root growth (Tsukagoshi *et al*. 2010).

Previously we reported that, in *Arabidopsis*, DSBs induce the early onset of endoreplication, in which DNA replication is repeated independently of mitosis or cytokinesis (Adachi *et al*. 2011). The transition from mitosis to endoreplication is accompanied by a rapid increase in cell size, and thus defines the boundary between the MZ and the EDZ in roots (Takatsuka & Umeda 2014). Indeed, DSBs cause meristematic cells to enter the EDZ, resulting in a reduction of meristem size (Adachi *et al*. 2011). We found that this phenomenon is a programmed response involving the SOG1-dependent signaling pathway, but how SOG1 regulates this transition to endoreplication in response to DNA damage remains unknown. As ROS distribution is important for the regulation of root meristem size, enzymes controlling ROS homeostasis are possible downstream targets of SOG1. In this study, we found that SOG1 directly induces the expression of *FMO1*, which encodes one of the flavin-containing monooxygenases of *Arabidopsis*. Our results showed that DSB-induced expression of *FMO1* leads to increased accumulation of H_2O_2 in the root tip, resulting in the reduction of meristem size and root growth inhibition. We propose that *de novo* ROS production is one of the major responses to DSBs mediated by the key transcription factor SOG1.

Results

DSBs promote H_2O_2 accumulation in the EDZ of *Arabidopsis* roots

To examine whether ROS homeostasis is affected by DNA damage in the root tip, we measured the levels of H_2O_2 and $O_2^{\bullet-}$ in *Arabidopsis* roots treated with the radiomimetic reagent zeocin, which induces DSBs (Berdy, 1980). Distribution of H_2O_2 and $O_2^{\bullet-}$ was visualized by staining tissues with the fluorescent indicators BES-H2O2-Ac and dihydroethidium (DHE), respectively (Maeda *et al*. 2004; Owusu-Ansah *et al*. 2009). In wild-type roots, the BES-H2O2-Ac fluorescence was detected in the EDZ, especially in the epidermis and the vasculature, but was very faint in the MZ, as reported previously (Tsukagoshi *et al*. 2010) (Fig. 1A). We found that 24 hr of treatment with 2 μM zeocin increased the fluorescence intensity in the EDZ, and expanded the fluorescent region into the apical region (Fig. 1A, C). On the other hand, the DHE fluorescence was observed in the MZ and the EDZ (Tsukagoshi *et al.* 2010), and was reduced by zeocin treatment (Fig. 1B, D), indicating the presence of reciprocal H_2O_2 and $O_2^{\bullet-}$ responses to DSBs. To identify the programmed response to DNA damage, we then observed the root tip of the *sog1-1* mutant, in which most of the events triggered by DSB-activated ATM are suppressed (Yoshiyama *et al.* 2009; 2013). Although the DHE fluorescence was reduced by zeocin treatment in a manner similar to that seen in the wild-type, the BES-H2O2-Ac fluorescence did not increase (Fig. 1). These results indicate that DSBs promote H_2O_2 accumulation in the EDZ in a SOG1-dependent manner, thereby reducing root meristem size.

SOG1 directly controls the expression of *FMO1*-encoding flavin-containing monooxygenase

The above results suggested that SOG1 controls H_2O_2 production in response to DNA damage, so we searched the *Arabidopsis* microarray database for genes involved in ROS synthesis whose expression levels are affected by DSBs. We found that *FMO1* (AGI code: AT1G19250) encoding flavin-containing monooxygenase and two putative glutathione-S-transferase (GST) genes (AT1G74590 and AT1G78340) are highly induced by γ irradiation, and that the induction is suppressed in *atm-1* and *sog1-1* mutants (Culligan *et al*. 2006; Yoshiyama *et al*. 2009). However, this suppression was not observed in the *atr* mutant (Culligan *et al*. 2006), suggesting that the ATM–SOG1 pathway controls *FMO1* and *GST* expressions in response to DSBs. Mishina & Zeier (2006) reported that ROS and salicylic acid synthesis induced by pathogen infection was suppressed in the *fmo1* mutant, supporting the involvement of *FMO1* in ROS homeostasis. We therefore focused on *FMO1* and monitored *FMO1* expression via quantitative RT-PCR, after treatment with 2 μM zeocin. The transcript level rapidly became elevated and reached its maximum after 12 hr; subsequently, expression rates decreased, and at 48 hr, returned to the same level as that detected prior to zeocin treatment (Fig. 2A). We found that, in *sog1-1*, zeocin-induced *FMO1* expression was not observed during these 48 hr (Fig. 2A), demonstrating that *FMO1* is induced by DSBs via the SOG1-mediated pathway.

We then tested whether SOG1 directly regulates *FMO1* expression. We used the transgenic line expressing *pSOG1::SOG1-MYC*, which can rescue *sog1-1* plants with

defects in DNA damage response (Yoshiyama *et al*. 2013). Chromatin immunoprecipitation (ChIP) was conducted using the anti-MYC antibody, and three genomic regions were amplified by PCR; namely, the 5'-promoter region (P1), the region around the transcription start site (P2), and the 3'-noncoding region (P3) (Fig. 2B). We found that the P2 region was highly enriched by ChIP when seedlings were treated with 2 μM zeocin for 24 hr (Fig. 2B). This indicates that DSB-activated SOG1 directly binds to the *FMO1* promoter and induces its expression.

The *fmo1* mutant is tolerant of DSBs

To reveal the function of *FMO1* in DNA damage response, we used the *fmo1* mutant with a T-DNA insertion in the 4th exon (Mishina & Zeier 2006). We measured root growth under DNA stress conditions: seedling grown on an MS medium for 5 days were transferred onto a medium containing 2 μM zeocin, and root length was measured for 6 days. There was no significant difference between the wild-type, *fmo1* and *sog1-1* in the absence of zeocin (Fig. 3A, B). However, when seedlings were treated with 2 μM zeocin, *fmo1* and *sog1-1* roots grew constantly, whereas in the wild-type, root growth was inhibited and almost stopped after 5 days (Fig. 3A, B).This result supports the idea that SOG1-controlled *FMO1* is involved in the inhibition of root growth in response to DSBs.

We also quantified root meristem size by counting the number of cortex cells between the quiescent center and the first elongated cell. We previously reported that zeocin treatment induces the early onset of endoreplication, thus promoting the

transition from cell division to cell elongation, and consequently restricting meristem size (Adachi *et al*. 2011; Takahashi *et al*. 2013). While the treatment of wild-type roots with 2 μM zeocin reduced meristem size by 42%, only a reduction of 19% and 11% was observed in *fmo1* and *sog1-1*, respectively (Fig. 3C, D). Lower sensitivity to zeocin as exhibited by root meristem size was also described previously (Adachi *et al*. 2011). These results indicate that *FMO1* is associated with controlling meristem size under DNA stress conditions.

FMO1 is required for alteration of H_2O_2 distribution upon DNA damage

To examine the spatial expression pattern of *FMO1*, we introduced the *pFMO1::FMO1-GFP* construct, which carries the 1.5 kb promoter and the coding region of *FMO1*, into the *fmo1* mutant. As shown in Figure S1A, the zeocin response in terms of root growth inhibition was recovered via expression of the transgene in *fmo1*, suggesting the functionality of the FMO1-GFP fusion protein. We found that, before starting zeocin treatment, GFP fluorescence was faintly observed in the vascular tissue of the EDZ (Fig. 4A). After 12 hr of zeocin treatment, fluorescence was detected in the epidermis of the MZ and the lateral root cap, and its expression in the vasculature spread to the MZ. Increased expression was observed over the MZ and EDZ afterwards (Fig. 4A, B). SOG1 is expressed in the MZ, and phosphorylated and activated upon DNA damage (Yoshiyama *et al.* 2013), supporting the idea that SOG1 induces the *FMO1* expression in the MZ after zeocin treatment. To test whether zeocin-induced expression of *FMO1* correlates with alteration in ROS distribution, we monitored the

H_2O_2 level after transferring seedlings onto a zeocin-containing medium. In the wild-type, the BES-H2O2-Ac fluorescence was detected only in the vasculature of the EDZ, but after 6 hr of zeocin treatment, the fluorescence intensity significantly increased and spread to the MZ (Fig. 4C, D). This is consistent with the above-mentioned result of the *FMO1-GFP* expression analysis. On the other hand, only a small increase in BES-H2O2-Ac fluorescence was observed in zeocin-treated *fmo1* after 48 hr (Fig. 4C, D). As expected, expression of *FMO1-GFP* rescued the impairment in H_2O_2 accumulation in zeocin-treated *fmo1* (Fig. S1B, C). These results suggest that the DSB-induced expression of *FMO1* is responsible for H_2O_2 accumulation, and changes in the distribution of H_2O_2 in the root tip.

Higher H_2O_2 accumulation in *FMO1*-overexpressing plants

To further understand the functional relevance of *FMO1* to the DNA damage response, we utilized transgenic lines overexpressing *FMO1* under the control of the 35S promoter (Koch *et al*. 2006). Semiquantitative RT-PCR showed that *FMO1* was highly expressed in the transgenic plants compared to expression levels in the wild-type, irrespective of the presence of zeocin (Fig. 5A). We found that *FMO1* overexpression delayed root growth in the absence of zeocin (Fig. 5B, C). This is probably due to higher levels of H_2O_2 accumulation, because BES-H2O2-Ac fluorescence was detected not only in the EDZ but also in the MZ; indeed, fluorescence intensity increased in the root tip (Fig. 5D, E). When plants were germinated on a medium containing 2 μM zeocin, root growth was arrested earlier in the transgenic line; namely, wild-type roots

stopped growing after 5-6 days, whereas *35S:FMO1* roots stopped growing after 4 days (Fig. 5B, C). In the root tip of *35S:FMO1* treated with zeocin, we observed the dramatic accumulation of H_2O_2 compared to that in the non-treated control (Fig. 5D, E). This indicates that DSBs still promote H_2O_2 accumulation when *FMO1* is overexpressed. These results suggest that SOG1 has other target(s) that promote H_2O_2 accumulation together with *FMO1,* and alter ROS homeostasis in roots under DNA stress conditions.

Discussion

Previous studies indicated that *Arabidopsis FMO1* is involved in the response to pathogen attack (Koch *et al*. 2006). In this study, we revealed a distinct function of *FMO1* involved in the control of root meristem size under DNA stress conditions. Our data demonstrated that *FMO1* is a direct target of SOG1, and is thus induced by the presence of damaged DNA. The *fmo1* mutant was tolerant of DSBs in terms of their effects on its root growth and meristem size; this phenotype was accompanied by a loss of DSB-induced H_2O_2 accumulation in the root tip. These results indicate that FMO1 is involved in the *de novo* synthesis of H_2O_2 downstream of SOG1, and is thereby involved in restricting root meristem size in response to DNA damage. Although transgenic plants overexpressing *FMO1* still exhibited the zeocin response, our data for the *fmo1* mutant clearly indicates that FMO1 functions as one of the major regulators governing H_2O_2 production under DNA stress conditions.

FMO1 is one of the flavin-containing monooxygenases (FMOs) which oxidize molecular oxygen using NADPH as an electron donor and FAD as a cofactor (Hines *et*

al. 1994). Koch *et al.* (2006) reported that *FMO1* expression was elevated in response to pathogen attack, and that the *fmo1* mutant exhibited enhanced susceptibility to pathogens. It is known that pathogen infection induces an oxidative burst and the production of ROS, which then trigger the expression of protective genes such as *glutathione S-transferase 1* (*GST1*), and trigger the hypersensitive response (Zeier *et al.* 2004). Indeed, no induction of *GST1* was observed in *fmo1* (Koch *et al*. 2006), indicating that FMO1 is required for ROS production in the hypersensitive response. Siddens *et al*. (2014) have recently reported that the expression of mammalian *FMO*s in insect cells led to the accumulation of H_2O_2 upon the addition of NADPH. This suggests that FMOs catalyze the synthesis of $O_2^{\bullet-}$, which is rapidly converted into more stable ROS such as H_2O_2, when a sufficient amount of SOD is present in the cells (Tynes *et al*. 1986). In *Arabidopsis* roots, $O_2^{\bullet-}$ and H_2O_2 preferentially accumulate in the MZ and the EDZ, respectively (Dunand *et al.* 2007). This study demonstrated that, under normal growth conditions, *FMO1* is faintly expressed in the vasculature of the EDZ, whereas zeocin treatment increased its expression and expanded the expression domain into the MZ. Therefore, it is likely that the DSB-induced expression of *FMO1* contributes to H_2O_2 accumulation in the EDZ rather than $O_2^{\bullet-}$ accumulation in the MZ, altering ROS homeostasis and reducing meristem size.

We previously showed that DSBs induce the early onset of endoreplication in *Arabidopsis,* and accelerate the transition from cell division to cell elongation (cell differentiation), thus reducing root meristem size (Adachi *et al*. 2011). Although this DNA damage response is dependent on SOG1, the underlying mechanisms were largely

unknown. Our microarray analysis using samples from *Arabidopsis* suspension cells revealed that zeocin up-regulated the expression of negative regulators of CDK activity, such as *CCS52A1*, *WEE1*, and the CDK inhibitors *SIM*, *SMR1*, and *SMR5* (Adachi *et al*. 2011). Moreover, many genes coding for cyclin A and B were down-regulated upon zeocin treatment. This observation is consistent with the currently accepted model of the onset of endoreplication; namely, when mitotic CDK activity is suppressed and never reaches the level necessary for progression from the G2 to the M phase, only DNA licensing and replication is repeated, leading to endoreplication (De Veylder *et al*. 2011). While Yi *et al*. (2014) recently reported that SOG1 directly induces the expression of *SMR5* and *SMR7;* SOG1 may also control other cell cycle-related genes by inducing *FMO1*. The previous report demonstrated that the oxidative stress caused by excess H_2O_2 suppressed expression of several cell cycle-related genes such as *CYCB1;1* and *CYCB1;2* in the MZ (Tsukagoshi *et al*. 2012). This suggests that *FMO1* is required for the *de novo* synthesis of ROS in response to DNA damage, which then down-regulate the expression of mitotic cyclin genes and promote the onset of endoreplication. The effect of ROS on cell cycle progression and cell fate has also been described in yeast and mammals (Muller 1991; Ranjan *et al.* 2006; Menon *et al.* 2003). On the other hand, it is also possible that ROS is involved in rapid cell elongation in the EDZ. In *Arabidopsis rhd2* mutants defective in the NADPH oxidase Atrboh C gene, root hairs burst at the transition to tip growth (Monshausen *et al*. 2007). Root hair bursting was also enhanced by scavenging ROS molecules in root tissue, suggesting that ROS production is associated with cell wall properties, which need to be properly controlled

during cell elongation (Monshausen *et al*. 2007).

The microarray data showed that the *FMO1* expression is under the control of ATM and SOG1, but not ATR, under DNA stress conditions (Culligan *et al.* 2006; Yoshiyama *et al.* 2009). This is consistent with our previous result indicating that endoreplication is induced by DSBs, but not directly by DNA replication stress (Adachi *et al*. 2011). In this study, we revealed that SOG1-mediated control of ROS homeostasis plays an important role in reducing root meristem size (Figure S2). Upon DSB induction, SOG1 is phosphorylated and activated by ATM. *FMO1* expression is then induced by SOG1, and H_2O_2 is accumulated in the EDZ of roots. Increased levels of H_2O_2 alter the expression of cell cycle-related genes and cell wall rigidity, thus promoting the onset of endoreplication and cell elongation. Consequently, meristem size is reduced, and root growth is delayed or arrested. Previous studies showed that *Arabidopsis* plants treated with salicylic acid exhibited a higher somatic recombination frequency (Lucht *et al.* 2002) and DNA damage response activation as a part of plant immune responses (Yan *et al.* 2013). Conversely, DNA-damaging agents, such as actinomycin D and mitomycin C, induce pathogenesis-related gene expression (Choi *et al.* 2001), as well as the expression of *RAD51D* and *BRCA2*, which function in DNA repair and control gene expression in response to pathogen infection (Wang *et al.* 2010). Considering these observations, SOG1-mediated control of *FMO1* may also be involved in immune responses. Further studies will reveal how external stresses induce DNA damage and affect ROS homeostasis, and how plants cope with environmental stresses by controlling organ growth and utilizing defense systems.

Experimental procedures

Plant materials and growth conditions

The mutant and transgenic lines were previously described: *fmo1* (Mishina & Zeier 2006), *35S::FMO1* (Koch *et al*. 2006), *sog1-1* (Yoshiyama *et al*. 2009), and *pSOG1::SOG1-MYC* (Yoshiyama *et al*. 2013). Plants were grown in Murashige and Skoog (MS) medium [0.5 x MS salts, 0.5 g/L 2-(N-morpholino) ethanesulfonic acid (MES), 1% (w/v) sucrose, and 0.4% phytoagar (pH 5.7)] under long-day conditions (16 hr light, 8 hr dark) at 22 °C.

ROS staining and microscopic observation

H_2O_2 and $O_2^{\bullet-}$ were visualized by staining tissues with BES-H2O2-Ac (Wako) and dihydroethidium (DHE) (Wako), respectively (Tsukagoshi *et al*. 2010). Plants were incubated in a liquid MS medium containing 5 μM BES-H2O2-Ac or 30 μM DHE for 30 min in the dark. After washing with an MS medium three times, fluorescent images were taken using a confocal laser scanning microscope (FV1000, Olympus), with a detection range of 485-515 nm for BES-H2O2-Ac and 510-550 nm for DHE. The fluorescence intensity was measured in the region 600 μm from the root tip using the Plot Profile function of the ImageJ software (Schneider *et al*. 2012).

RT-PCR

Total RNA was extracted from *Arabidopsis* roots using an RNeasy Plant Mini Kit

(QIAGEN). First-strand cDNAs were prepared from total RNA using the Superscript II First-Strand Synthesis System (Invitrogen), according to the manufacturer's instructions. Quantitative PCR was performed using a THUNDERBIRD SYBR qPCR Mix (TOYOBO) with 100 nM primers and 0.1 μg of first-strand cDNA. PCR reactions were conducted using the LightCycler 480 Real-Time PCR System (Roche) according to the following conditions: 95 °C for 5 min; 45 cycles at 95 °C for 10 sec, at 60 °C for 10 sec, and at 72 °C for 15 sec. *ACTIN2* (At3g18780) was used as a reference gene. Primer sequences are listed in Table S1.

Chromatin immunoprecipitation

A ChIP experiment was performed as previously described (Saleh *et al*. 2008), with minor modifications. Using 1.5 g of 10-day-old *pSOG1::SOG1-MYC* roots, chromatin bound to SOG1 proteins was precipitated using the anti-MYC antibody (Santa Cruz Biotechnology). Primers for real-time quantitative PCR were designed to amplify DNA fragments of 100 to 200 bp (Table S1).

Expression analysis of *FMO1*

The *FMO1* genomic fragment, which carries an 1.5 kb promoter region upstream of the transcription start site and the coding region, was amplified via PCR with the primers listed in Table S1, and subcloned into the modified pGWB4 vector (Nakagawa *et al.* 2009) to generate a binary vector harboring the fusion construct with *GFP* (*pFMO1::FMO1-GFP*). The construct was introduced into the *fmo1* mutant, and the

resulting transgenic lines were observed with a confocal laser scanning microscope. To visualize cell outlines, seedlings were stained with 0.1 mg/ml propidium iodide (PI), according to the method described by Truernit & Haseloff (2008), with minor modifications.

Measurement of root meristem size

Roots were stained with 0.1 mg/ml PI and observed with a confocal laser scanning microscope. The number of cortex cells between the quiescent center and the first elongated cell was counted (Perilli *et al*. 2010).

Acknowledgements

We would like to thank Anne B. Britt, Kaoru O. Yoshiyama, and Nikolaus L. Schlaich for seeds of the *sog1-1, pSOG1::SOG1-MYC* and *35S::FMO1* lines, respectively. We also wish to thank Naoki Takahashi for his critical reading of this manuscript. This work was supported by MEXT KAKENHI (Grant Number 22119009), JSPS KAKENHI (Grant Number 26291061) and JST, CREST.

References

Adachi, S., Minamisawa, K., Okushima, Y., Inagaki, S., Yoshiyama, K., Kondou, Y., Kaminuma, E., Kawashima, M., Toyoda, T., Matsui, M., Kurihara, D., Matsunaga, S. & Umeda, M. (2011) Programmed induction of endoreduplication by DNA double-strand breaks in *Arabidopsis*. *Proc. Natl. Acad. Sci. USA*. **108**, 10004–10009.

Berdy, J. (1980) Bleomycin-type antibiotics. In: *Amino Acid and Peptide Antibiotics – Handbook of Antibiotic Compounds,* IV (1) (eds J. Berdy), pp. 459–497. Boca Raton, FL: CRC Press.

Choi, J.J., Klosterman, S.J. & Hadwiger, L.A. (2001) A comparison of the effects of DNA-damaging agents and biotic elicitors on the induction of plant defense genes, nuclear distortion, and cell death. *Plant Physiol.* **125**, 752–762.

Culligan, K.M., Tissier, A. & Britt, A.B. (2004) ATR regulates a G2-phase cell-cycle checkpoint in *Arabidopsis thaliana*. *Plant Cell* **16**, 1091–1104.

Culligan, K.M., Robertson, C.E., Foreman, J., Doerner, P. & Britt, A.B. (2006) ATR and ATM play both distinct and additive roles in response to ionizing radiation. *Plant J.* **48**, 947–961.

De Veylder, L., Larkin, J.C. & Schnittger, A. (2011) Molecular control and function of endoreplication in development and physiology. *Trends Plant Sci.* **16**, 624–634.

Dunand, C., Crèvecoeur, M. & Penel, C. (2007) Distribution of superoxide and hydrogen peroxide in *Arabidopsis* root and their influence on root development: possible interaction with peroxidases. *New Phytol.* **174**, 332–341.

Foreman, J., Demidchik, V., Bothwell, J.H.F., Mylona, P., Miedema, H., Torres, M.A., Linstead, P., Costa, S., Brownlee, C., Jones, J.D.G., Davies, J.M. & Dolan, L. (2003) Reactive oxygen species produced by NADPH oxidase regulate plant cell growth. *Nature* **422**, 442–446.

Garcia, V., Bruchet, H., Camescasse, D., Granier, F., Bouchez, D. & Tissier, A. (2003) AtATM is essential for meiosis and the somatic response to DNA damage in plants. *Plant Cell* **15**, 119–132.

Harper, J.W. & Elledge, S.J. (2007) The DNA damage response: ten years after. *Mol. Cell* **28**, 739–745.

Hines, R.N., Cashman, J.R., Philpot, R.M., Williams, D.E. & Ziegler, D.M. (1994) The mammalian flavin-containing monooxygenases: molecular characterization and regulation of expression. *Toxicol. Appl. Pharmacol.* **125**, 1–6.

Koch, M., Vorwerk, S., Masur, C., Sharifi-Sirchi, G., Olivieri, N. & Schlaich, N.L. (2006) A role for a flavin-containing mono-oxygenase in resistance against microbial pathogens in *Arabidopsis*. *Plant J.* **47**, 629–639.

Kovtun, Y., Chiu, W.L., Tena, G. & Sheen, J. (2000) Functional analysis of oxidative stress-activated mitogen-activated protein kinase cascade in plants. *Proc. Natl. Acad. Sci. USA*. **97**, 2940–2945.

Lucht, J.M., Mauch-Mani, B., Steiner, H.Y., Metraux, J.P., Ryals, J. & Hohn, B. (2002) Pathogen stress increases somatic recombination frequency in *Arabidopsis*. *Nature Genet.* **30**, 311–314.

Maeda, H., Fukuyasu, Y., Yoshida, S., Fukuda, M., Saeki, K., Matsuno, H., Yamauchi,

Y., Yoshida, K., Hirata, K. & Miyamoto, K. (2004) Fluorescent probes for hydrogen peroxide based on a non–oxidative mechanism. *Angew. Chem. Int. Ed. Engl.* **43**, 2389–2391.

Menon, S.G., Sarsour, E.H., Spitz, D.R., Higashikubo, R., Sturm, M., Zhang, H. & Goswami, P.C. (2003) Redox regulation of the G1 to S phase transition in the mouse embryo fibroblast cell cycle. *Cancer Res.* **63**, 2109–2117.

Mishina, T.E. & Zeier, J. (2006) The Arabidopsis flavin-dependent monooxygenase FMO1 is an essential component of biologically induced systemic acquired resistance. *Plant Physiol.* **141**, 1666–1675.

Monshausen, G.B., Bibikova, T.N., Messerli, M.A., Shi, C. & Gilroy, S. (2007) Oscillations in extracellular pH and reactive oxygen species modulate tip growth of *Arabidopsis* root hairs. *Proc. Natl. Acad. Sci. USA.* **104**, 20996–21001.

Muller, E.G. (1991) Thioredoxin deficiency in yeast prolongs S phase and shortens the G1 interval of the cell cycle. *J. Biol. Chem.* **266**, 9194–9202.

Mur, L.A., Kenton, P. & Draper, J. (2005) In planta measurements of oxidative bursts elicited by avirulent and virulent bacterial pathogens suggests that H_2O_2 is insufficient to elicit cell death in tobacco. *Plant Cell Environ*. **28**, 548–561.

Nakagawa, T., Ishiguro, S. & Kimura, T. (2009) Gateway vectors for plant transformation. *Plant Biotech.* **26**, 275–284.

Nezames, C.D., Sjogren, C.A., Barajas, J. F. & Larsen, P.B. (2012) The *Arabidopsis* cell cycle checkpoint regulators TANMEI/ALT2 and ATR mediate the active process of aluminum-dependent root growth inhibition. *Plant Cell* **24**, 608–621.

Owusu-Ansah, E. & Banerjee, U. (2009) Reactive oxygen species prime *Drosophila* haematopoietic progenitors for differentiation. *Nature* **461**, 537–541.

Perilli, S., Moubayidin, L. & Sabatini, S. (2010) The molecular basis of cytokinin function. *Curr. Opin. Plant Biol.* **13**, 21–26.

Potocky, M., Jones, M.A., Bezvoda, R., Smirnoff, N. & Zarsky, V. (2007) Reactive oxygen species produced by NADPH oxidase are involved in pollen tube growth. *New Phytol.* **174**, 742–751.

Ranjan, P., Anathy, V., Burch, P.M., Weirather, K., Lambeth, J.D. & Heintz, N.H. (2006) Redox-dependent expression of *cyclin D1* and cell proliferation by Nox1 in mouse lung epithelial cells. *Antioxid. Redox Signal.* **8**, 1447–1459.

Roldán-Arjona, T. & Ariza, R.R. (2009) Repair and tolerance of oxidative DNA damage in plants. *Mutat. Res.* **681**, 169–179.

Reeves, E.P., Lu, H., Jacobs, H.L., Messina, C.G.M., Bolsover, S., Gabella, G., Potma, E.O., Warley, A., Roes, J. & Segal, A.W. (2002) Killing activity of neutrophils is mediated through activation of proteases by K^+ flux. *Nature* **416**, 291–297.

Riballo, E., Kühne, M., Rief, N., Doherty, A., Smith, G.C., Recio, M.J. & Löbrich, M. (2004) A pathway of double-strand break rejoining dependent upon ATM, Artemis, and proteins locating to γ-H2AX foci. *Mol. Cell* **16**, 715–724.

Riley, T., Sontag, E., Chen, P. & Levine, A. (2008) Transcriptional control of human *p53*-regulated genes. *Nature Rev. Mol. Cell Biol.* **5**, 402–412.

Saleh, A., Alvarez-Venegas, R. & Avramova, Z. (2008) An efficient chromatin immunoprecipitation (ChIP) protocol for studying histone modifications in

Arabidopsis plants. *Nature Protoc.* **3**, 1018–1025.

Sakamoto, T., Inui, Y.T., Uraguchi, S., Yoshizumi, T., Matsunaga, S., Mastui, M., Umeda, M., Fukui, K. & Fujiwara, T. (2011) Condensin II alleviates DNA damage and is essential for tolerance of boron overload stress in *Arabidopsis*. *Plant Cell* **23**, 3533–3546.

Schneider, C.A., Rasband, W.S. & Eliceiri, K.W. (2012) NIH image to ImageJ: 25 years of image analysis. *Nature Methods* **9,** 671–675.

Shiotani, B. & Zou, L. (2009) Single-stranded DNA orchestrates an ATM-to-ATR switch at DNA breaks. *Mol. Cell* **33**, 547–558.

Siddens, L.K., Krueger, S.K., Henderson, M.C. & Williams, D.E. (2014) Mammalian flavin-containing monooxygenase (FMO) as a source of hydrogen peroxide. *Biochem. Pharmacol.* **89**, 141–147.

Takahashi, N., Kajihara, T., Okamura, C., Kim, Y., Katagiri, Y., Okushima, Y. & Umeda, M. (2013) Cytokinins control endocycle onset by promoting the expression of an APC/C activator in *Arabidopsis* roots. *Curr. Biol.* **23**, 1812–1817.

Takatsuka, H. & Umeda, M. (2014) Hormonal control of cell division and elongation along differentiation trajectories in roots. *J. Exp. Bot.* **65**, 2633–2643.

Takeda, S., Gapper, C., Kaya, H., Bell, E., Kuchitsu, K. & Dolan, L. (2008) Local positive feedback regulation determines cell shape in root hair cells. *Science* **319**, 1241–1244.

Tanaka, T., Halicka, H.D., Huang, X., Traganos, F. & Darzynkiewicz, Z. (2006) Constitutive histone H2AX phosphorylation and ATM activation, the reporters of

DNA damage by endogenous oxidants. *Cell Cycle* **5**, 1940–1945.

Torres, M.A., Dangl, J.L. & Jones, J.D.G. (2002) *Arabidopsis* gp91^{phox} homologues *AtrbohD* and *AtrbohF* are required for accumulation of reactive oxygen intermediates in the plant defense response. *Proc. Natl. Acad. Sci. USA*. **99**, 517–522.

Truernit, E. & Haseloff, J. (2008) A simple way to identify non-viable cells within living plant tissue using confocal microscopy. *Plant Methods* **4**, 15.

Tsukagoshi, H., Busch, W. & Benfey, P.N. (2010) Transcriptional regulation of ROS controls transition from proliferation to differentiation in the root. *Cell* **143**, 606–616.

Tsukagoshi, H. (2012) Defective root growth triggered by oxidative stress is controlled through the expression of cell cycle-related genes. *Plant Sci.* **197**, 30–39.

Tynes, R.E., Sabourin, P.J., Hodgson, E. & Philpot, R.M. (1986) Formation of hydrogen peroxide and N-hydroxylated amines catalyzed by pulmonary flavin-containing monooxygenases in the presence of primary alkylamines. *Arch. Biochem. Biophys.* **251**, 654–664.

Wang, S., Durrant, W.E., Song, J., Spivey, N.W. & Dong, X. (2010) *Arabidopsis* BRCA2 and RAD51 proteins are specifically involved in defense gene transcription during plant immune responses. *Proc. Natl. Acad. Sci. USA*. **107**, 22716–22721.

Yan, S., Wang, W., Marqués, J., Mohan, R., Saleh, A., Durrant, W.E. & Dong, X. (2013) Salicylic acid activates DNA damage responses to potentiate plant immunity.

Mol. Cell **52**, 602–610.

Yi, D., Kamei, C.L.A., Cools, T., Vanderauwera, S., Takahashi, N., Okushima, Y., Eekhout, T., Yoshiyama, K.O., Larkin, J., Van den Daele, H., Conklin, P., Britt, A., Umeda, M. & De Veylder, L. (2014) The *Arabidopsis* SIAMESE-RELATED cyclin-dependent kinase inhibitors SMR5 and SMR7 regulate the DNA damage checkpoint in response to reactive oxygen species. *Plant Cell* **26**, 296–309.

Yoshiyama, K., Conklin, P.A., Huefner, N.D. & Britt, A.B. (2009) Suppressor of gamma response 1 (SOG1) encodes a putative transcription factor governing multiple responses to DNA damage. *Proc. Natl. Acad. Sci. USA*. **106**, 12843–12848.

Yoshiyama, K.O., Kobayashi, J., Ogita, N., Ueda, M., Kimura, S., Maki, H. & Umeda, M. (2013) ATM-mediated phosphorylation of SOG1 is essential for the DNA damage response in *Arabidopsis*. *EMBO Rep.* **14**, 817–822.

Zeier, J., Pink, B., Mueller, M.J. & Berger, S. (2004) Light conditions influence specific defence responses in incompatible plant–pathogen interactions: uncoupling systemic resistance from salicylic acid and PR-1 accumulation. *Planta* **219**, 673–683.

Zhou, B.B. & Elledge, S.J. (2000) The DNA damage response: putting checkpoints in perspective. *Nature* **408**, 433–439.

Figure legends

Figure 1. ROS distribution in the root tip.

(A and B) Fluorescence images of root tips stained with BES-H2O2-Ac (A) or DHE (B). Five-day-old seedlings of the wild-type and *sog1-1* were transferred onto a medium with or without 2 μM zeocin, and grown for 24 hr. Bars = 100 μm. (C and D) Fluorescence intensity observed in (A) and (B), respectively. Black and grey bars indicate the values of samples treated without or with zeocin, respectively. Values shown are relative to the wild-type grown in the absence of zeocin. Data are presented as mean ± SD (n = 10). Significant differences from the control grown in the absence of zeocin were determined by Student's *t*-test: *, $P < 0.05$.

Figure 2. SOG1 directly controls *FMO1* expression.

(A) *FMO1* expression after zeocin treatment. Five-day-old seedlings of the wild-type and *sog1-1* were treated with 2 μM zeocin for the lengths of time indicated. Transcript levels were measured via qRT-PCR and normalized to that of *ACTIN2*. The expression levels are given as relative values, with that for plants prior to zeocin treatment set to 1. Data are presented as mean ± SD (n = 3). (B) ChIP-PCR analysis. The genomic structure of *FMO1* is shown; open and black boxes indicate non-coding and coding regions, respectively, and the arrow represents the transcription start site. Transgenic plants harboring *pSOG1::SOG1-MYC* were treated with or without 2 μM zeocin for 24 hr, and ChIP was conducted using anti-MYC antibodies. The genomic fragments amplified by qPCR are shown in the schematic diagram (P1, P2, and P3). Black and

grey bars indicate the values of samples treated without or with zeocin, respectively. Values relative to the non-treated control are represented as mean ± SD (n = 3). Significant differences from the non-treated control were determined by Student's *t*-test: *, $P < 0.05$.

Figure 3. The *fmo1* mutant is tolerant to zeocin.

(A) Wild-type, *fmo1* and *sog1-1* seedlings grown in the absence or presence of zeocin. Five-day-old seedlings were transferred onto a medium with or without 2 μM zeocin and grown for 6 days. Bar = 1 cm. (B) Root growth of seedlings is shown in (A). Data are presented as mean ± SD (n = 30). Significant differences from the wild-type were determined by Student's *t*-test: *, $P < 0.05$. (C) Root tips of the wild-type, *fmo1,* and *sog1-1*. Six-day-old seedlings were treated with or without 2 μM zeocin for 24 hr, and root tips were made observable via staining with propidium iodide. Blue and white arrowheads indicate the QC and the first elongated cell in the cortex cell file, respectively. Bar = 100 μm. (D) Cortex cell number in the meristematic zone of the seedlings is shown in (C). Black and grey bars indicate the cell numbers of samples treated without or with zeocin, respectively. Data are presented as mean ± SD (n = 30). Significant differences from the non-treated control were determined by Student's *t*-test: *, $P < 0.05$.

Figure 4. *FMO1* controls H_2O_2 accumulation under DNA stress conditions.

(A) *FMO1* expression in response to zeocin. Five-day-old seedlings harboring *pFMO1::FMO1-GFP* were transferred onto a medium containing 2 μM zeocin, and grown for the time periods indicated. Bar = 100 μm. (B) GFP fluorescence intensity observed in (A). The fluorescence intensities are indicated as relative values, with those of plants prior to zeocin treatment set to 1. Data are presented as mean ± SD (n = 10). (C) H_2O_2 accumulation in response to zeocin. Five-day-old seedlings of wild-type and *fmo1* were transferred onto a medium containing 2 μM zeocin, and grown for the time periods indicated. Then, the seedlings were stained with BES-H2O2-Ac. Bar = 100 μm. (D) Fluorescence intensity is presented in (C). The fluorescence intensities are presented as relative values, with that for the wild-type before zeocin treatment set to 1. Data are presented as mean ± SD (n = 10). Significant differences from plants prior to zeocin treatment were determined by Student's *t*-test: *, $P < 0.05$.

Figure 5. Phenotype of *FMO1*-overexpressing plants.

(A) RT-PCR analysis of *FMO1*. Five-day-old seedlings of the wild-type and *35S::FMO1* were transferred onto a medium with or without 2 μM zeocin, and grown for 24 hr. Total RNA was extracted from roots and subjected to RT-PCR. *ACTIN2* was used as a control. (B) Seedlings of the wild-type and *35S::FMO1*. Five-day-old seedlings were transferred onto a medium with or without 2 μM zeocin, and grown for 6 days. Bar = 1 cm. (C) Root growth of the wild-type and *35S::FMO1*. Five-day-old seedlings were transferred onto a medium with or without 2 μM zeocin, and root length was measured for 6 days. Data are presented as mean ± SD (n = 30). Significant

differences from the wild-type were determined by Student's *t*-test: *, $P < 0.05$. (D) H_2O_2 accumulation in the wild-type and *35S::FMO1*. Five-day-old seedlings were transferred onto a medium with or without 2 μM zeocin, and grown for 24 hr. Then, the seedlings were stained with BES-H2O2-Ac. Bar = 100 μm. (E) Fluorescence intensity presented in (D). Black and grey bars indicate the values of samples treated without or with zeocin, respectively. The fluorescence intensities are indicated as relative values, with that for the non-treated wild-type set to 1. Data are presented as mean ± SD (n = 10). Bars with different letters differ significantly from each other ($P < 0.05$).

Supporting information

Figure S1. Root phenotype of *fmo1* harboring *pFMO1::FMO1-GFP*.

Figure S2 Model for the control of root meristem size under DNA stress conditions.

Table S1. Primers used for cloning, RT-PCR and ChIP assay.

Figure 1

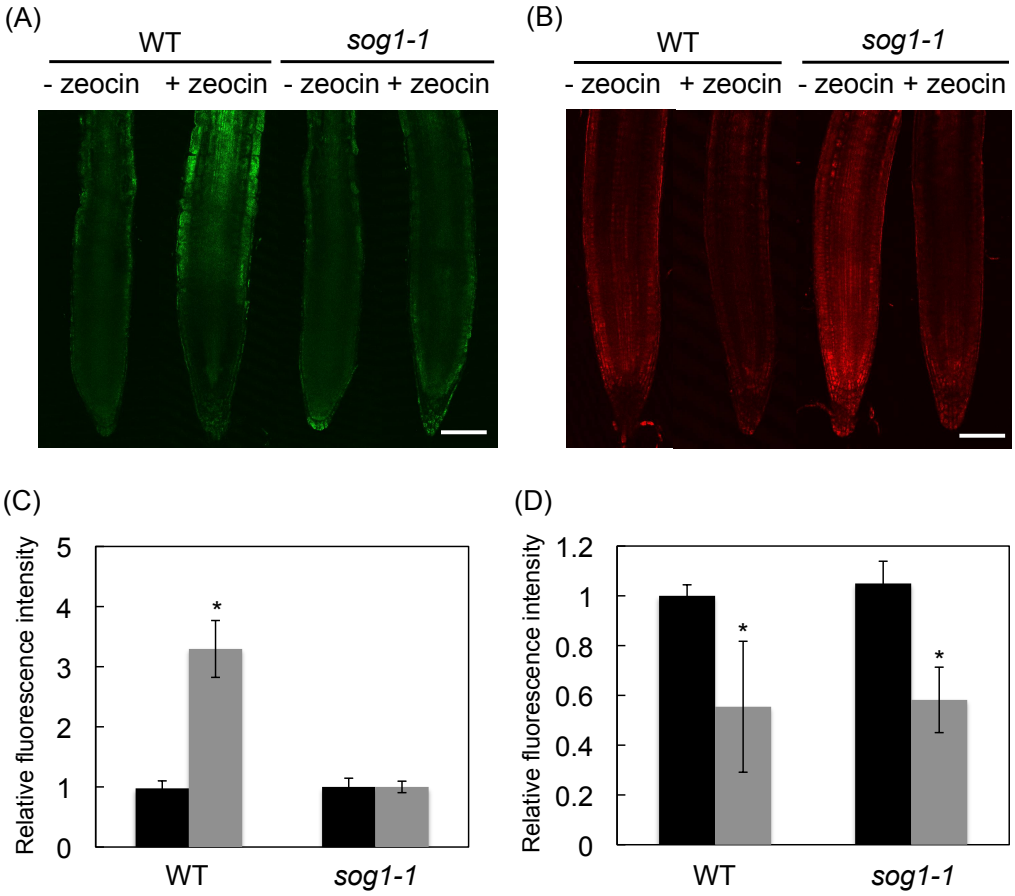
(A)
WT
sog1-1
- zeocin
+ zeocin
- zeocin
+ zeocin
(B)
WT
sog1-1
- zeocin
+ zeocin
- zeocin
+ zeocin
(C)
Relative fluorescence intensity
0
1
2
3
4
5
*
WT
sog1-1
(D)
Relative fluorescence intensity
0
0.2
0.4
0.6
0.8
1
1.2
*
*
WT
sog1-1

Figure 2

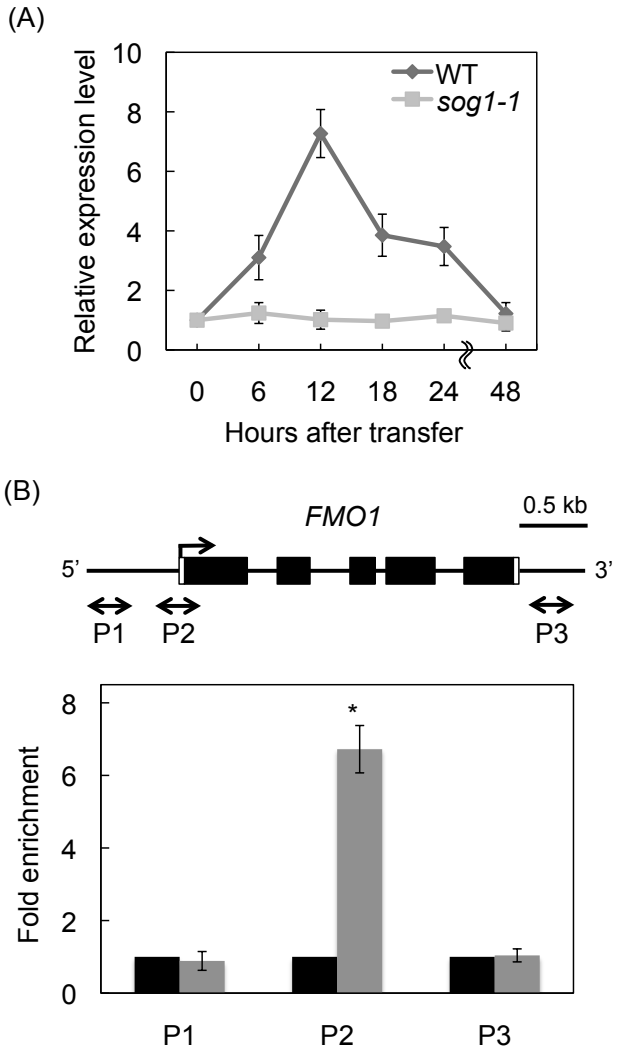
(A)
Relative expression level
10
8
6
4
2
0
WT
sog1-1
0
6
12
18
24
48
Hours after transfer
(B)
FMO1
0.5 kb
5'
3'
P1
P2
P3
Fold enrichment
8
6
4
2
0
*
P1
P2
P3

Figure 3

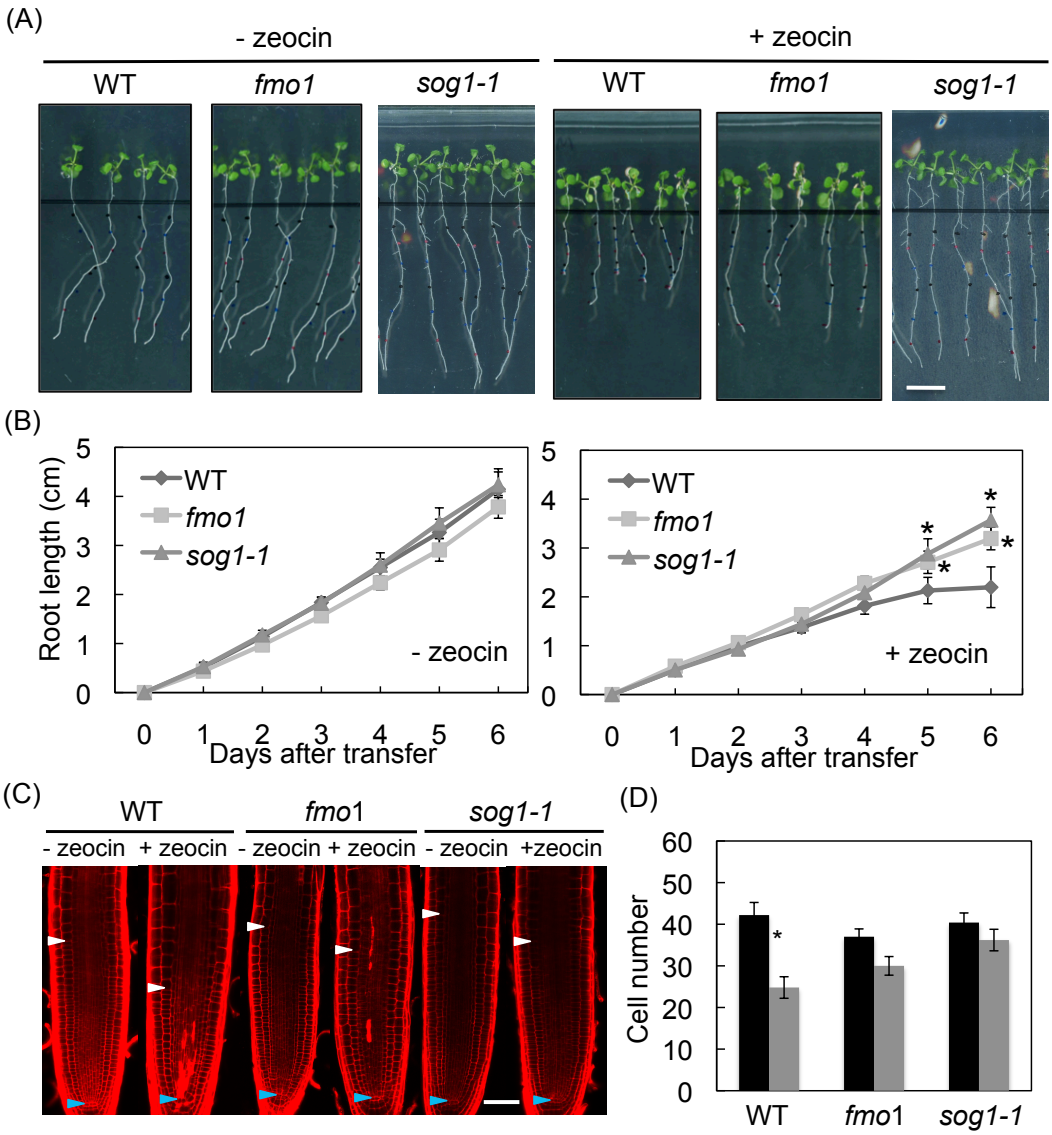
(A)
- zeocin
+ zeocin
WT
fmo1
sog1-1
WT
fmo1
sog1-1
(B)
Root length (cm)
Days after transfer
WT
fmo1
sog1-1
- zeocin
+ zeocin
(C)
WT
fmo1
sog1-1
- zeocin + zeocin
- zeocin +zeocin
(D)
Cell number
WT
fmo1
sog1-1

Figure 4

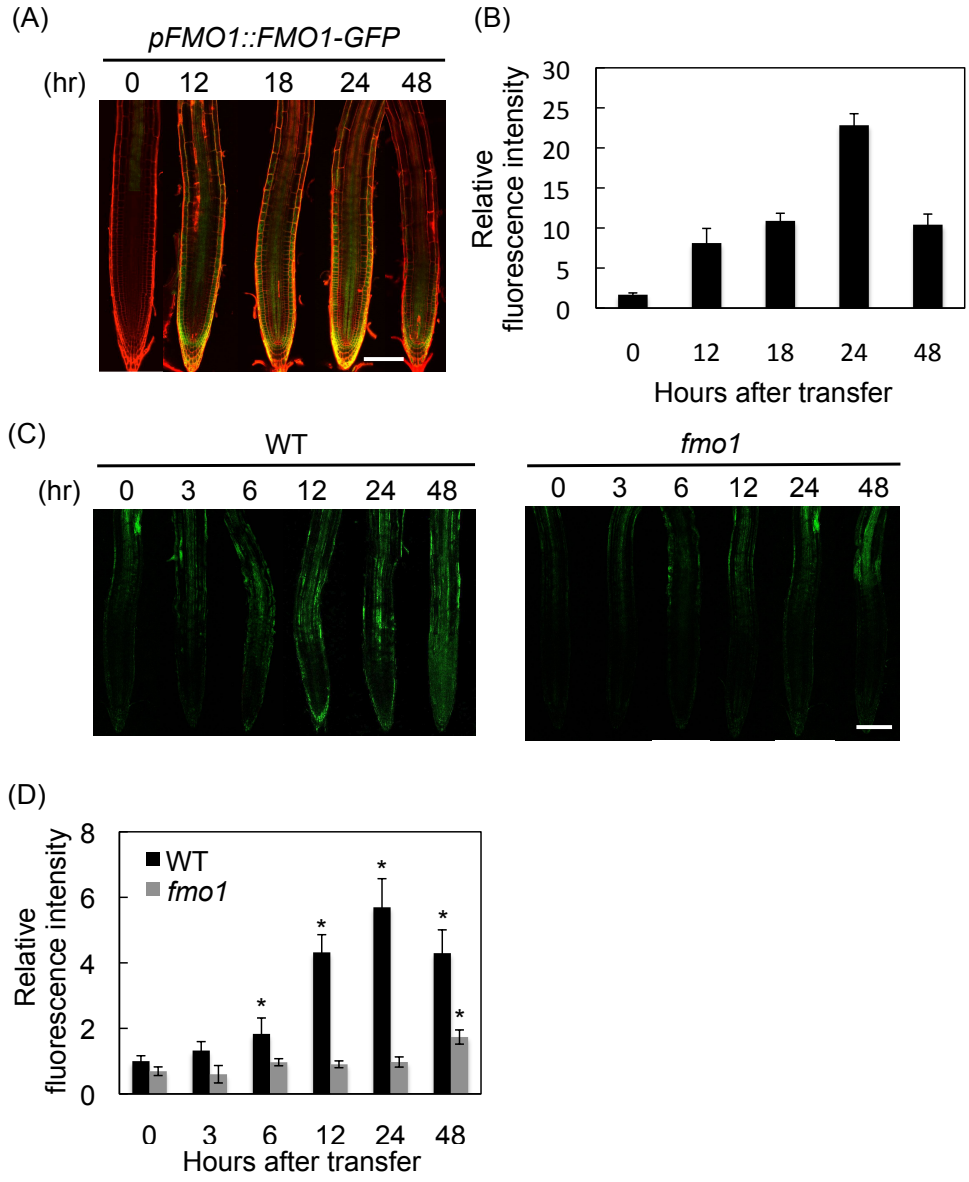
(A)
pFMO1::FMO1-GFP
(hr) 0 12 18 24 48
(B)
Relative fluorescence intensity
30
25
20
15
10
5
0
0 12 18 24 48
Hours after transfer
(C)
WT
fmo1
(hr) 0 3 6 12 24 48
0 3 6 12 24 48
(D)
Relative fluorescence intensity
8
6
4
2
0
WT
fmo1
*
0 3 6 12 24 48
Hours after transfer

Figure 5

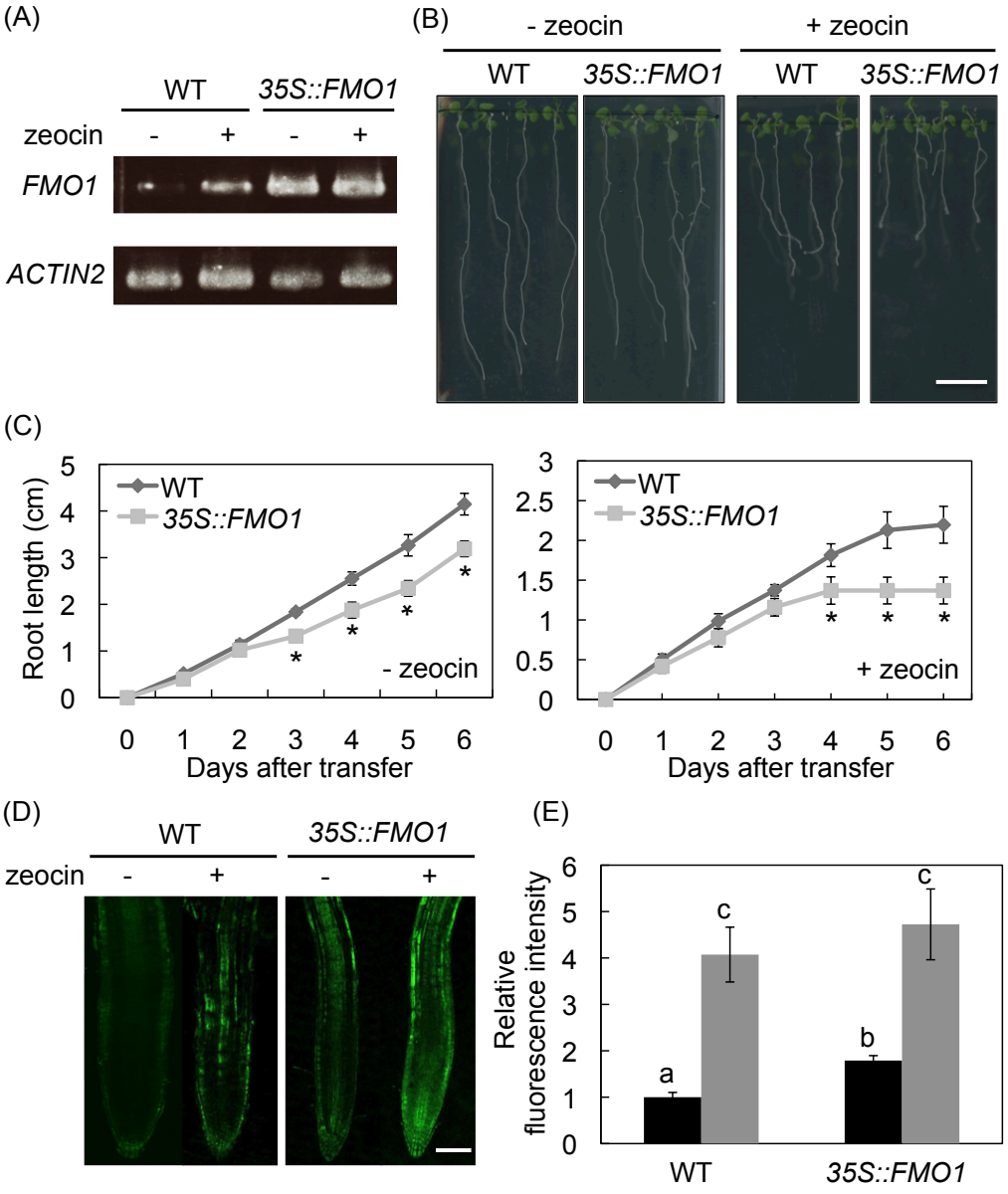
(A)
WT
35S::FMO1
zeocin
- + - +
FMO1
ACTIN2
(B)
- zeocin
+ zeocin
WT
35S::FMO1
WT
35S::FMO1
(C)
Root length (cm)
WT
35S::FMO1
- zeocin
+ zeocin
Days after transfer
Days after transfer
(D)
WT
35S::FMO1
zeocin
- + - +
(E)
Relative fluorescence intensity
a
b
c
c
WT
35S::FMO1

Table S1. Primers used for cloning, RT-PCR and ChIP assay

Cloning	
FMO1	5’- AAAAAGCAGGCTCCATGGCTTCTAACTATGATAAG -3’ 5’- TGTACAAAGTGGCAGCAGTCATATCTTCTTT -3’
pFMO1::FMO1	5’- AAAAAGCAGGCTCCAGTTCAAGAACCTGACAG -3’ 5’- TGTACAAAGTGGCAGCAGTCATATCTTCTTT -3’
RT-PCR	
FMO1	5’- TAAGGTCTTACCCGGCAGGACTGAT -3’ 5’- CTGATGAGGTTTGAGCAACTGAACC -3’
ACTIN2	5’- GGCTCCTCTTAACCCAAAGGC -3’ 5’- CACACCATCACCAGAATCCAGC -3’
ChIP assay	
P1	5’- CGGAAAAACAAACATTTTCCCG -3’ 5’- GGATAGTTGTTTATCGAGAAAT -3’
P2	5’- CGCTTGCAGAAATTTCCTCACA -3’ 5’- GCTAGAGAGAAGAGATTAATG -3’
P3	5’- CGTTAGAAAGCTCTCGGAAAAA -3’ 5’- CGAGAGCTTTCTAACGTTTAAG -3’

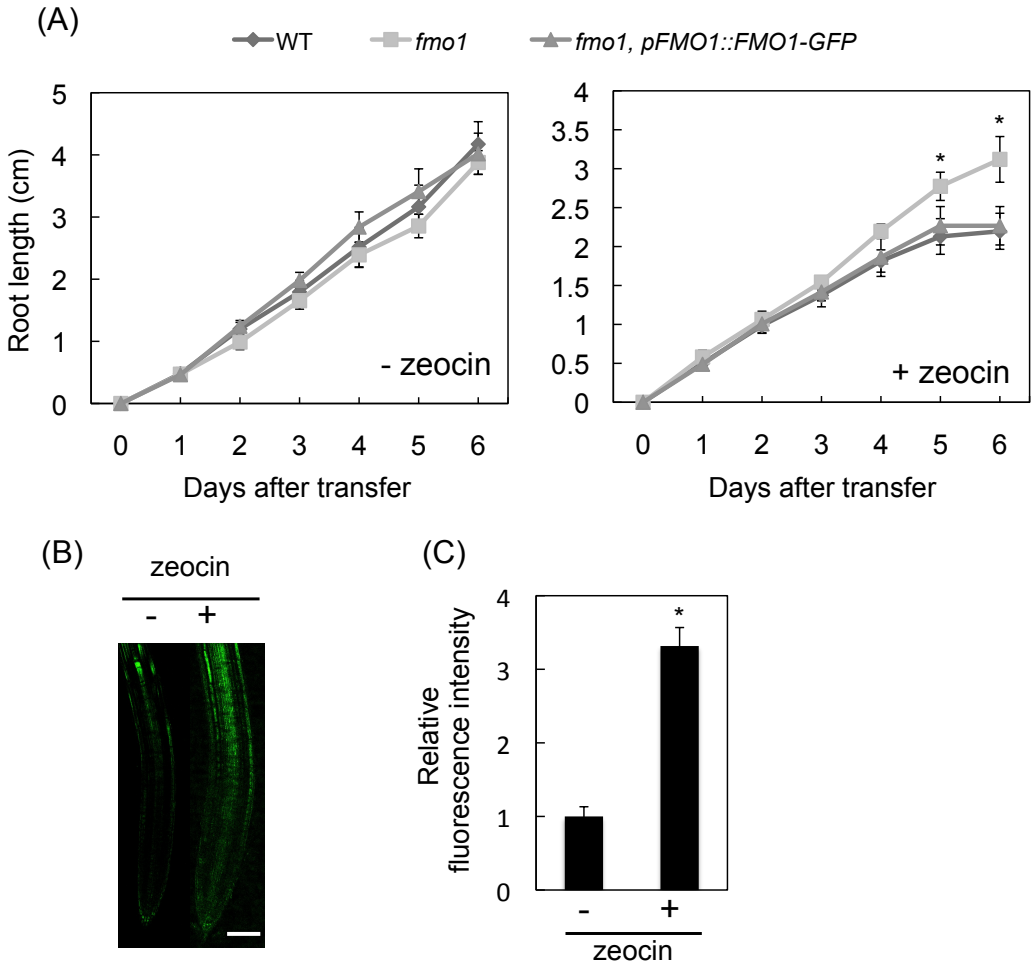

Figure S1. Root phenotype of *fmo1* harboring *pFMO1::FMO1-GFP*.

(A) Five-day-old seedlings of the wild-type, *fmo1*, and *fmo1* harboring *pFMO1::FMO1-GFP* were transferred onto a medium with or without 2 μM zeocin, and root length was measured for 6 days. Data are presented as mean ± SD (n = 30). Significant differences from the wild-type were determined by Student's *t*-test: *, $P < 0.05$. (B) Five-day-old *fmo1* seedlings harboring *pFMO1::FMO1-GFP* were transferred onto a medium with or without 2 μM zeocin, and grown for 24 hr. Then, the seedlings were stained with BES-H2O2-Ac. Bar = 100 μm. (C) Fluorescence intensity presented in (B). The fluorescence intensities are indicated as relative values, with those of non-treated plants set to 1. Data are presented as mean ± SD (n = 10). The significant difference from the non-treated control was determined by Student's *t*-test: *, $P < 0.05$.

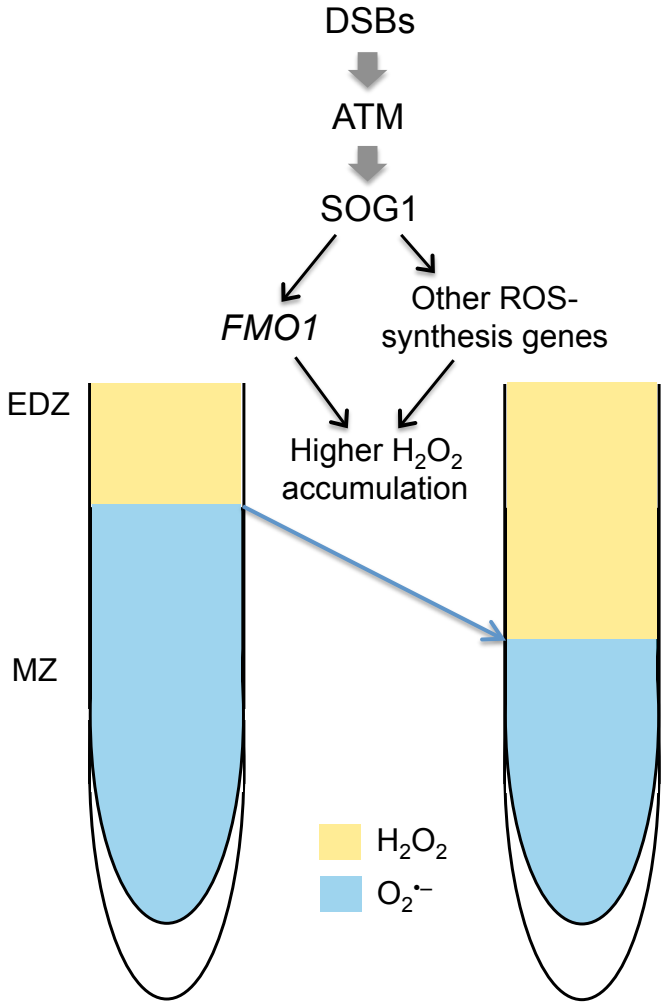

Figure S2. Model for the control of root meristem size under DNA stress conditions.

SOG1 induces the expression of *FMO1* and other ROS-synthesis genes, leading to the increased accumulation of H_2O_2. As a result, the balance of $H_2O_2/O_2^{\bullet-}$ changes, and the root meristem size is reduced. EDZ, elongation/differentiation zone; MZ, meristematic zone.